

Construction of Tricyclic Nitrogen Heterocycles by Gold(I)-Catalyzed Cascade Cyclization of Allenynes and Its Application to Polycyclic π -Electron Systems

Hiroki Komatsu,^[a] Takaya Ikeuchi,^[a] Hitomi Tsuno,^[a] Norihito Arichi,^[a] Kosuke Yasui,^[b] Shinya Oishi,^[a] Shinsuke Inuki,^[a] Aiko Fukazawa,^{*[b]} and Hiroaki Ohno^{*[a]}

[a] H. Komatsu, T. Ikeuchi, H. Tsuno, Dr. N. Arichi, Prof. Dr. S. Oishi, Prof. Dr. S. Inuki, Prof. Dr. H. Ohno
Graduate School of Pharmaceutical Sciences
Kyoto University
Sakyo-ku, Kyoto 606-8501 (Japan)
E-mail: hohno@pharm.kyoto-u.ac.jp

[b] Dr. K. Yasui, Prof. Dr. A. Fukazawa
Institute for Integrated Cell-Material Sciences (WPI-iCeMS)
Institute for Advanced Study
Kyoto University
Sakyo-ku, Kyoto 606-8501 (Japan)
E-mail: afukazawa@icems.kyoto-u.ac.jp

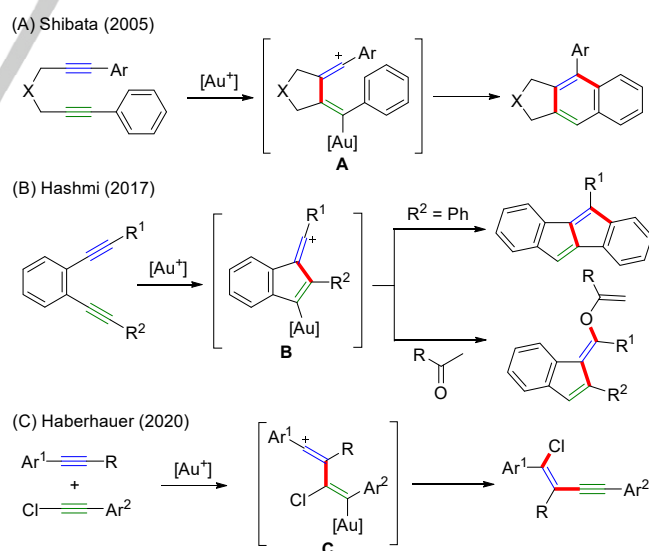
Supporting information: Reaction optimization, X-ray crystallography of **5a** and **21**, quantum chemical calculations of **3a** and **3g**, SAPT analysis and optical properties of **21**, and experimental procedures, including characterization data, for all new compounds.

Abstract: A novel approach to the direct construction of tricyclic nitrogen heterocycles based on gold-catalyzed cascade cyclization of aminoallenynes is described. The expected bis-cyclization reaction of hydroxyisobutryl-protected aminoallenynes was efficiently promoted by a catalytic amount of BrettPhosAuNTf₂ in the presence of *i*PrOH, producing 1,2-dihydrobenzo[*cd*]indole derivatives in good yields. Combined with Friedel–Crafts acylation or palladium-catalyzed *N*-arylation, the resulting tricyclic products were efficiently converted to nitrogen-containing polycyclic aromatic compounds (N-PACs) with highly conjugated π -electron systems. The newly obtained hexacyclic indolium salts showed characteristic concentration-dependent absorption and emission properties.

Introduction

Gold complexes are strong π -Lewis acids that can activate carbon–carbon multiple bonds to facilitate various transformations of alkynes, including cascade cyclization reactions to produce complex molecules.^[1,2] Recent progress in highly reactive gold catalysts has shown that alkynes can function as nucleophiles toward carbon–carbon multiple bonds to form vinyl cation species^[3] that are useful for further transformations. In 2005, Shibata disclosed an interesting gold-catalyzed cascade cyclization of 1,6-diyne derivatives, leading to formal [4 + 2] adducts (Scheme 1A).^[4] This reaction can be rationalized by the formation of vinyl cation species **A**, which is trapped by the neighboring aryl group. In 2017, Hashmi reported gold-catalyzed bis-cyclization reactions of diynes to produce pentalenes, fulvenes, and related carbocycles, proceeding through vinyl cation intermediate **B** (Scheme 1B).^[5] The intermolecular coupling of diynes is also useful for carbocycle synthesis.^[5d,e] Haberhauer reported a gold-catalyzed intermolecular reaction of chloroalkynes with an internal alkyne to form vinyl cation species **C**, which produces chloroenyne derivatives via migration of the chlorine substituent (Scheme 1C).^[6] Furthermore, vinyl cation

formation using ynamide-containing diynes^[7] or gold carbenoids (derived from alkyne oxidation),^[8] and gold vinylidene complex formation using a terminal alkyne,^[9] have been widely investigated. However, to our knowledge, gold-catalyzed vinyl cation formation involving amine-type nitrogen nucleophiles is unprecedented. This can be partly attributed to the generally higher nucleophilicity of amino groups compared with alkynes, which would inhibit the formation of vinyl cation species by promoting alkyne hydroamination.^[10]

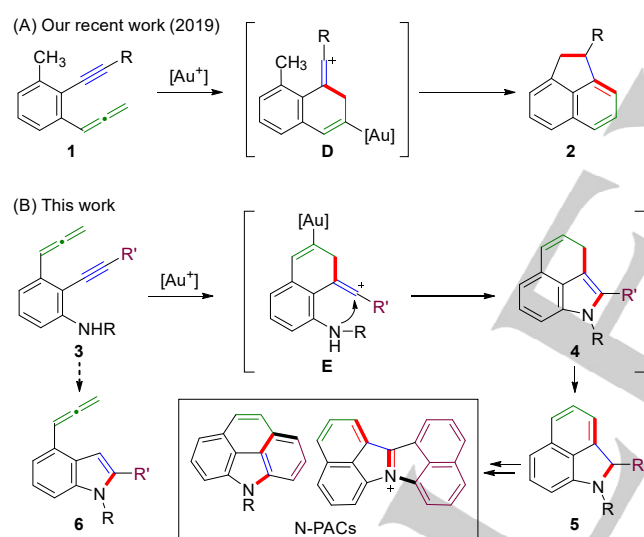


Scheme 1. Gold(I)-catalyzed reactions of diynes and related compounds proceeding through vinyl cation intermediates.

Recently, we reported a gold-catalyzed reaction of allenyne **1** to give acenaphthene **2** via the formation of vinyl cation **D** and carbocyclization with the methyl group (Scheme 2A).^[11,12] Based

RESEARCH ARTICLE

on this reaction, we designed a gold-catalyzed cascade reaction of allenes using a nitrogen functional group as the nucleophile for vinyl cation species to construct benzo[*cd*]indole scaffolds (Scheme 2B),^[13] which are present in many biologically active compounds, including ergot alkaloids. Accordingly, coordination of a gold complex to the allene moiety in **3** facilitates the formation of vinyl cation **E** via nucleophilic attack of the internal alkyne to the activated allene. Subsequent nucleophilic cyclization via the nitrogen nucleophile would produce tricyclic fused indole **4** or pyrrolonaphthalene **5** through double-bond isomerization. Key to the success of this strategy was suppression of the aforementioned nucleophilic cyclization through reaction of the nitrogen functional group with the activated alkyne to produce allenylindole **6**. We expected to overcome this undesirable process by appropriate selection of nitrogen functional groups and optimization of the reaction conditions. Herein, we describe a successful gold-catalyzed cascade cyclization of aminoallenes **3** to produce pyrrolonaphthalenes **5** using an unusual hydroxylated acyl protecting group. Several nitrogen-containing polycyclic aromatic compounds (N-PACs)^[14] could be readily synthesized from the resulting pyrrolonaphthalenes. Among them, the polycyclic indolium ion showed characteristic concentration-dependent absorption/emission properties owing to strong intermolecular interactions.

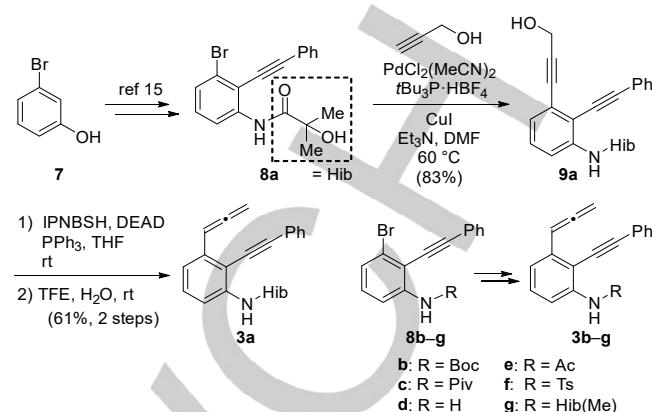


Scheme 2. Our work: Gold(I)-catalyzed cascade cyclizations of allenes.

Results and Discussion

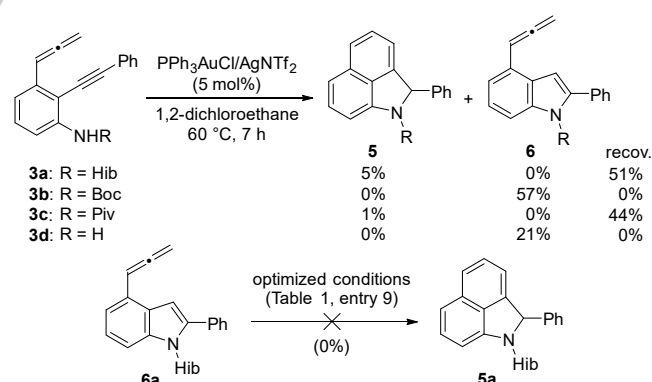
The preparation of aminoallenes **3** is shown in Scheme 3. Known alkynyl bromoaniline derivative **8a** bearing a 2-hydroxyisobutyryl (Hib) group was synthesized according to the literature.^[15] This bromoaniline bearing the unusual protecting group was directly converted to the cyclization precursor **3a** without changing the protecting group, which later led us to unexpected good results. Thus, Sonogashira coupling of **8a** with propargyl alcohol gave diyne **9a**, which was converted to Hib-protected aminoallene **3a** by using Movassaghi–Myers deoxygenation.^[16] Aminoallenes **3b–g** possessing different *N*-protecting groups were prepared from **8b–g**. Other

aminoallenes were also prepared in a similar manner (see the Supporting information).



Scheme 3. Preparation of substrates. Boc = *tert*-butoxycarbonyl, DEAD = diethyl azodicarboxylate, DMF = *N,N*-dimethylformamide, Hib = 2-hydroxyisobutyryl, Hib(Me) = 2-methoxyisobutyryl, IPNBSh = *N*-isopropylidene-*N'*-2-nitrobenzenesulfonyl hydrazine, TFE = 2,2,2-trifluoroethanol, Ts = *p*-toluenesulfonyl.

With protected aminoallenes **3** in hand, we examined the gold-catalyzed reaction using *in-situ*-prepared $\text{PPh}_3\text{AuNTf}_2$ (5 mol%) in 1,2-dichloroethane (Scheme 4). The reactions of Hib- and Piv-protected aminoallenes **3a** and **3c** gave the desired bis-cyclization products **5**, albeit in low yields (5% and 1%, respectively). In contrast, the reactions of Boc-protected and unprotected substrates **3b** and **3d** gave allenylindoles **6** without promoting the desired bis-cyclization. The structure of **5a** was confirmed by X-ray crystallography (see the Supporting information). Notably, reacting identically prepared allenylindole **6a** under the optimized conditions (see Table 1, entry 9) did not produce pyrrolonaphthalene **5a**, suggesting that **6a** was not the intermediate of bis-cyclization.^[17]

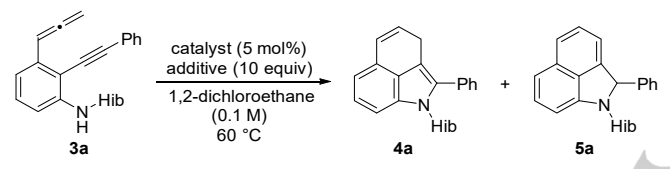


Scheme 4. Initial attempts of gold(I)-catalyzed cascade cyclization and treatment of **6a** under the optimized conditions. Yields were determined by ¹H NMR analysis. Tf = trifluoromethanesulfonyl.

Next, the reaction conditions were optimized using Hib-protected substrate **3a** (Table 1). First, several ligands were screened in the reaction in 1,2-dichloroethane at 60 °C (entries 1–3 and Supporting information). The reaction using IPrAuCl

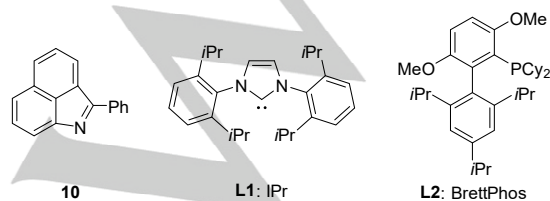
RESEARCH ARTICLE

(L1AuCl) gave pyrrolonaphthalene **5a** in a significantly improved yield (39%, entry 2). Similarly, the reaction in the presence of BrettPhosAuNTf₂ provided fused indole **4a** and pyrrolonaphthalene **5a** in 45% and 15% yields, respectively (entry 3). As purification of **4a** was difficult owing to its susceptibility to oxidation, we focused on improving the yield of more-stable pyrrolonaphthalene **5a**. When the reaction using BrettPhosAuNTf₂ was conducted for 24 h, **5a** was obtained as the sole isolable isomer in 51% yield (entry 4). This result suggested that fused indole **4a** was isomerized to pyrrolonaphthalene **5a** under the reaction conditions. As silver salt might promote the isomerization in entries 1 and 2 (producing **5a** within 7 h),^[18] we tested the conditions using additional AgNTf₂, which improved the yield of **5a** to 62% (entry 6). However, the desired cyclization reaction was not promoted by silver salt alone (entry 7). Finally, the addition of *i*PrOH (to promote protodeauration)^[19] and use of an argon atmosphere (to suppress oxidation) improved the yield of **5a** to 75% (entry 9). Under the optimized conditions, the reaction was also reproduced on a 1-mmol scale (entry 10).

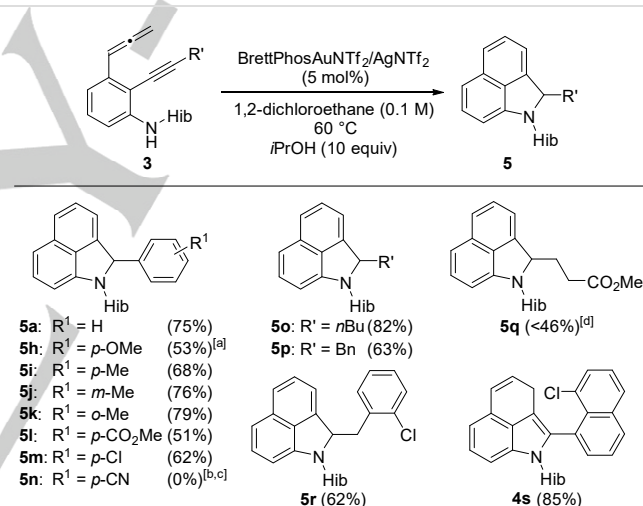
Table 1. Optimization of reaction conditions.


Entry	Catalyst	Time [h]	Additive	Yield [%] ^[a]		Recov. [%]
				4a ^[b]	5a	
1	PPh ₃ AuCl/AgNTf ₂	7	–	0	5	51
2	L1AuCl/AgNTf ₂	7	–	0	39	0
3	L2AuNTf ₂	7	–	45	15	0
4	L2AuNTf ₂	24	–	0	51	0
5	L2AuCl/AgNTf ₂	7	–	0	54	2
6	L2AuNTf ₂ /AgNTf ₂	7	–	0	62	0
7	AgNTf ₂	7	–	0	0	20
8	L2AuNTf ₂ /AgNTf ₂	6	<i>i</i> PrOH	0	71	0
9 ^[c]	L2AuNTf ₂ /AgNTf ₂	5	<i>i</i> PrOH	0	75 (73) ^[d]	0
10 ^[c,e]	L2AuNTf ₂ /AgNTf ₂	9	<i>i</i> PrOH	0	75 ^[d]	0

[a] Determined by ¹H NMR analysis. [b] Product **4a** was gradually converted to compound **10** on silica gel. [c] Conducted under Ar. [d] Isolated yields. [e] Reaction performed on a 1 mmol scale. Cy = cyclohexyl.



With optimized conditions in hand (Table 1, entry 9), we investigated the reaction scope using various substrates bearing different substituents at the alkyne terminus (Table 2). Aminoallenynes **3** bearing electron-donating groups (OMe, Me) or electron-withdrawing groups (CO₂Me, Cl) at the *p*-position of the terminal phenyl group reacted smoothly to afford corresponding pyrrolonaphthalenes **5h**, **5i**, **5l**, and **5m** in 51–68% yields. The position of methyl group on the terminal phenyl group did not affect the reaction significantly, with desired products **5j** and **5k** produced in good yields (76–79%). Using substrate **3n** bearing a cyano group, substrate degradation occurred to give only a complex mixture of unidentified products. Alkyl substituents at the alkyne terminus, such as *n*-butyl, benzyl, functionalized alkyl, and chlorobenzyl groups, were well tolerated, affording desired pyrrolonaphthalenes **5o**–**5r**. Interestingly, when a chloronaphthyl-substituted substrate was used, fused indole derivative **4s** without double-bond isomerization was obtained as the sole isolated isomer, presumably due to the highly conjugated system derived from the naphthyl group. These results indicated that the reaction had sufficient substrate scope for alkyne substituents.

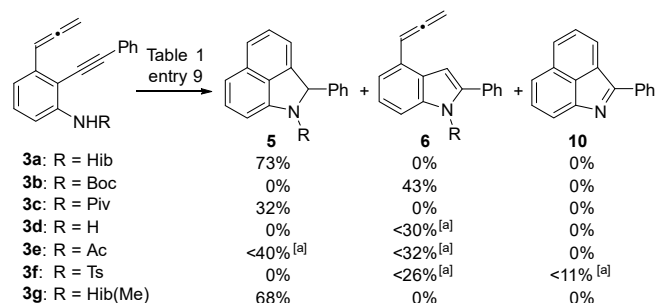
Table 2. Substrate scope.

[a] Oxidized byproduct was obtained. [b] Complex mixture. [c] Reaction was conducted at 0.05 M. [d] Containing a small amount of impurities.

As anticipated, the nitrogen substituent showed significant limitations (Scheme 5). Acyl protecting groups, such as pivaloyl and acetyl groups, afforded decreased yields of desired products **5** (32–40%; **5c** and **5e**). Furthermore, the desired reaction did not proceed using substrates **3b**, **3d**, and **3f** bearing an unprotected or Boc/Ts-protected amino group, yielding allenylindoles **6**, as well as a small amount of oxidized product **10** when using **3f**. These results showed that appropriate choice of the nitrogen substituent was crucial for this reaction, with the Hib group proving particularly useful. Notably, when the corresponding methylated protecting group [Hib(Me)] was used in this reaction, a comparable yield of pyrrolonaphthalene **5g** was obtained (68%), suggesting that an oxygen atom in the protecting group, rather than a free hydroxy group, plays an important role in this reaction. At the present stage of our understandings, the details of the effect of the Hib and Hib(Me) groups on this reaction efficacy remain unclear. In light of the fact that Boc-protected **3b** and the unprotected **3d** preferentially underwent alkyne hydroamination to

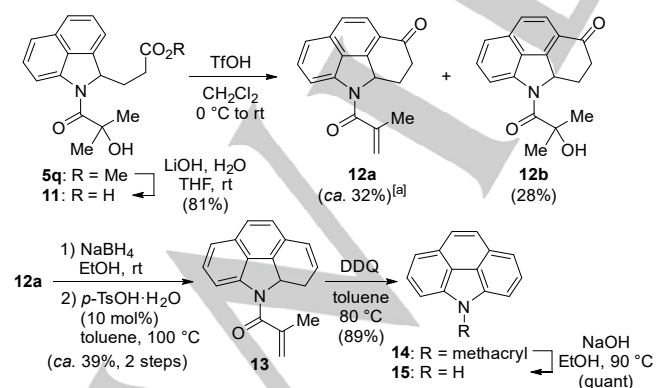
RESEARCH ARTICLE

form **6**, the Hib and Hib(Me) groups should play a crucial role for the suppression of this reaction pathway. The intramolecular hydrogen bonding with a N–H proton^[20] as well as the proton-transfer ability due to the basicity of the oxygen atom,^[19b] and/or steric bulk of the Hib or Hib(Me) group can contribute to the reactivity and selectivity.



Scheme 5. Effect of nitrogen protecting group (after reaction optimization). [a] Containing a small amount of impurities.

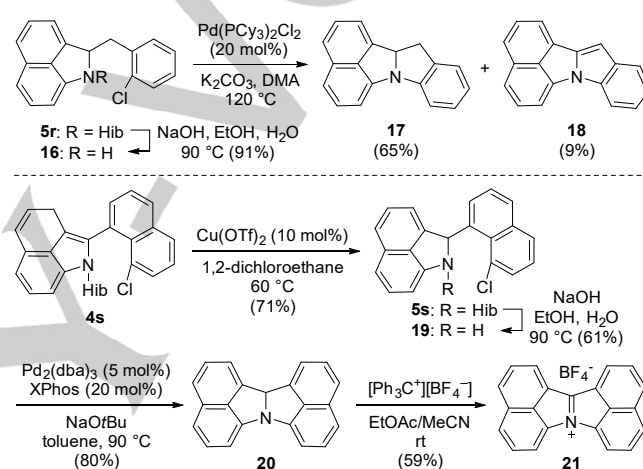
Taking advantage of this cyclization reaction, the thus obtained pyrrolonaphthalene moieties were further applied to the synthesis of nitrogen-containing polycyclic aromatic compounds (N-PACs). As N-PACs are expected to have different electrochemical and optical properties compared with the corresponding polyaromatic hydrocarbons (PAHs), their precise synthesis is particularly significant in materials chemistry.^[14] First, we investigated construction of the 4*H*-benzo[*def*]carbazole skeleton^[21] by intramolecular Friedel–Crafts acylation (Scheme 6). Hydrolysis of **5q** and intramolecular Friedel–Crafts acylation of resulting acid **11** using TfOH gave a mixture of tetracyclic compounds **12a** and **12b**. According to the reported protocol,^[22] the reduction of ketone **12a**, followed by hydroxy-group elimination accompanied by aromatization, gave **14** bearing the 4*H*-benzo[*def*]carbazole skeleton. Hydrolysis of the amide then afforded 4*H*-benzo[*def*]carbazole **15**.^[23] Although the intramolecular acylation step requires further improvement,^[24] this synthesis has potential utility for producing substituted 4*H*-benzo[*def*]carbazole derivatives.



[a] Containing a small amount of impurities.

Scheme 6. Synthesis of N-PACs via intramolecular Friedel–Crafts acylation.

Next, we attempted the synthesis of fused aza-acenaphthene analogues through intramolecular *N*-arylation (Scheme 7). Removal of the Hib group from pyrrolonaphthalene **5r** bearing an *ortho*-chlorobenzyl group, followed by palladium-catalyzed intramolecular *N*-arylation, afforded pentacyclic compound **17** (65%) and its oxidized form **18** (9%). To obtain a N-PAC with a more π -expanded framework, we also investigated using corresponding naphthyl derivative **4s** as a key precursor in the synthesis. Copper-catalyzed double-bond isomerization of fused indole **4s** to the corresponding naphthalene **5s** and successive deprotection of the Hib group, followed by palladium-catalyzed intramolecular *N*-arylation, led to hexacyclic compound **20**. Finally, treatment of **20** with triphenylmethylium tetrafluoroborate^[25] gave indolium salt **21**. Notably, compound **21** exhibited sufficient stability that enabled handling under ambient conditions without any precautions.



Scheme 7. Synthesis of N-PACs via intramolecular *N*-arylation. DMA = *N,N*-dimethylacetamide.

Among the N-PACs obtained in this study, indolium salt **21** showed characteristic solid-state packing and concentration-dependent photophysical properties. X-ray crystallographic analysis of indolium salt **21** showed that the rigid hexacyclic framework exhibited almost planar geometry, with dihedral angles between the two naphthalene moieties of 2.15° and 2.32° for two crystallographically independent units (Figure 1a). This planar hexacyclic framework formed dense π -stacked arrays, in which the molecules were displaced in a zigzag pattern along their longer axes (Figure 1b). The molecules in an identical π -stacked array had substantial face-to-face overlap with close proximity. Specifically, the intermolecular C \cdots C distances of C15 \cdots C32, C39 \cdots C48, and C13 \cdots C45 were 3.372, 3.315, and 3.344 Å, respectively, all of which were shorter than the sum of van der Waals radii of the carbon atoms (3.40 Å).^[26] Zeroth-order symmetry-adaptive perturbation theory (SAPT0) calculations for the dimeric structure extracted from the packing structures using the jun-cc-pVDZ basis set^[27,28] showed that significant stabilization by dispersion forces was likely crucial for formation of the densely π -stacked structure (Figure S8). The offset arrangement of π -planes, with the electron-deficient iminium moiety and the electron-rich naphthalene rings in close proximity

Table 2. Concentration effect of the photophysical properties of **21** in CH₃CN.

Conc. [M] ^[a]	λ_{abs} [nm] ^[b] (ϵ [M ⁻¹ cm ⁻¹]) ^[c]	λ_{fl} [nm] ^[d]	$\Delta\nu$ [cm ⁻¹] ^[e]	Φ_f ^[f]	τ [ns] ^[g]	k_r [10 ⁷ s ⁻¹] ^[h]	k_{nr} [10 ⁷ s ⁻¹] ^[i]
1.0×10^{-4}	488 (2.81×10^4) 376 (9.10×10^3)	624	4500	0.13	10.7	1.2	8.1
1.0×10^{-6}	323 (1.39×10^4)	440	8300	0.09	2.7	3.3	34

[a] Sample concentration in CH₃CN. [b] Absorption maximum wavelength. [c] Molar extinction coefficient. [d] Fluorescence maximum wavelength. [e] Stokes shift. [f] Absolute fluorescence quantum yield determined using an integrated sphere system. [g] Fluorescence lifetime. [h] Radiative rate constant. [i] Nonradiative rate constant.

to each other, should also play a vital role in reducing exchange repulsion at least in part.

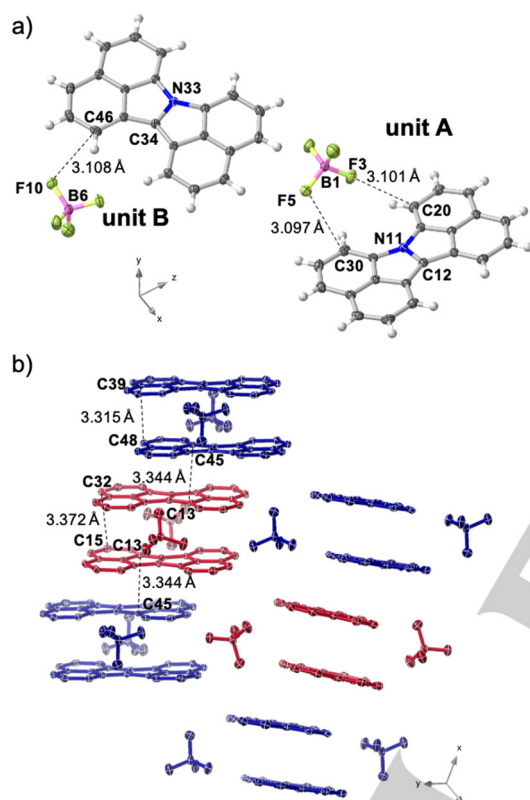


Figure 1. X-ray crystal structure of **21** (50% probability for thermal ellipsoids). (a) Monomolecular and (b) bimolecular lattice structures.

Reflecting the strong intermolecular interaction, polycyclic indolium ion **21** exhibited significantly concentration-dependent photophysical properties in CH₃CN (Table 3). In the absorption spectra, the longest-wavelength absorption band with an absorption maximum wavelength (λ_{abs}) of 323 nm diminished when the solution concentration was increased from 1.0×10^{-6} M to 1.0×10^{-4} M, and new absorption bands emerged at λ_{abs} of 488 and 376 nm, with an isosbestic point at around 350 nm (Figure 2a). Furthermore, the fluorescence of **21** showed a substantial red-shift from a fluorescence maximum wavelength (λ_{fl}) of 440 nm to 624 nm with increasing concentration (Figure 2b). Notably, a substantial decrease in the Stokes shift from 8300 cm⁻¹ to 4500 cm⁻¹, and an increase in the fluorescence quantum yield (Φ_f) from 0.09 to 0.13, were observed with increasing concentration. These

results reflected the formation of ground-state aggregates in a higher-concentration solution in CH₃CN.^[29] Notably, polycyclic indolium ion **21** can form such aggregates at a relatively low concentration of 10^{-4} M, even without substituents such as long alkyl chains or hydrogen-bonding functional groups, which are frequently used to furnish secondary intermolecular interactions. This result might be attributed to the strong intermolecular interaction between polycyclic indolium ion moieties, although the structure of the aggregates remained unclear.

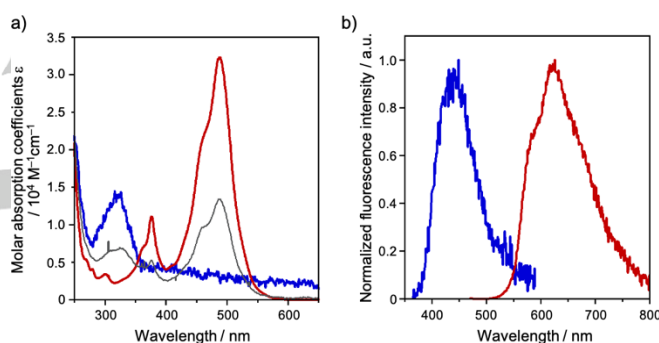


Figure 2. (a) UV-Vis absorption and (b) fluorescence spectra of indolium salt **21** in CH₃CN at concentrations of 1.0×10^{-6} M (blue), 1.0×10^{-5} M (gray), and 1.0×10^{-4} M (red).

Conclusion

We have developed a gold-catalyzed cascade cyclization of aminoallenynes for the direct construction of pyrrolonaphthalene scaffolds. Key to the success of this reaction was the use of an unusual protecting group, namely, hydroxyisobutyryl (Hib) group or its methylated congener. To our knowledge, this is the first example of an amine-type nitrogen nucleophile being used in a gold-catalyzed reaction involving vinyl cation formation. During the course of our application study for the synthesis of N-PACs, a polycyclic indolium salt with highly planar π -electron systems was obtained, which exhibited characteristic concentration-dependent photophysical properties attributable to aggregate formation, even without any additional substituents.

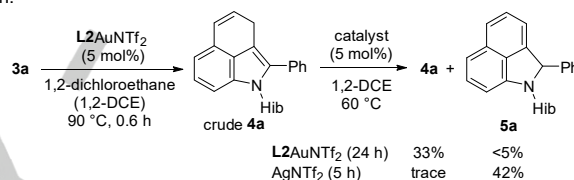
Acknowledgements

This work was supported by the JSPS KAKENHI (17H03971 for H.O., and 20H05864 for A.F.), AMED (Grant Numbers 20gm1010007h0004 and 20am0101092j0004), and the Tokyo Biochemical Research Foundation (TBRF). The authors are

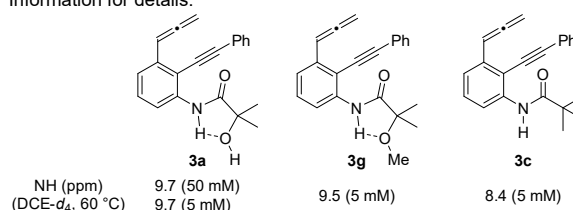
grateful to Prof. S. Kitagawa (iCeMS, Kyoto University) for providing access to an X-ray single crystal diffractometer, and Prof. A. Wakamiya and Dr. T. Nakamura (ICR, Kyoto University) for the measurement of absolute fluorescence quantum yields and time-resolved fluorescence spectra. The authors also thank Mr. M. Hayakawa (Nagoya University) for his assistance with the X-ray crystallographic analysis of **21**.

Keywords: gold catalysis • vinyl cation • domino reaction • N-PAC • fluorescence emission

- [1] For selected reviews on gold catalysis, see: a) D. J. Gorin, F. D. Toste, *Nature* **2007**, *446*, 395–403; b) A. S. K. Hashmi, M. Rudolph, *Chem. Soc. Rev.* **2008**, *37*, 1766–1775; c) Y. Li, W. Li, J. Zhang, *Chem. Eur. J.* **2017**, *23*, 467–512.
- [2] For selected reviews on gold-catalyzed cascade reactions, see: a) H. Ohno, *Isr. J. Chem.* **2013**, *53*, 869–882; b) J. L. Mascareñas, I. Varela, F. López, *Acc. Chem. Res.* **2019**, *52*, 465–479.
- [3] M. Niggemann, S. Gao, *Angew. Chem. Int. Ed.* **2018**, *57*, 16942–16944; *Angew. Chem. Int. Ed.* **2018**, *130*, 17186–17188.
- [4] T. Shibata, R. Fujiwara, D. Takano, *Synlett* **2005**, 2062–2066.
- [5] a) T. Wurm, J. Bucher, S. B. Duckworth, M. Rudolph, F. Rominger, A. S. K. Hashmi, *Angew. Chem.* **2017**, *129*, 3413–3417; *Angew. Chem. Int. Ed.* **2017**, *56*, 3364–3368; b) T. Wurm, J. Bucher, M. Rudolph, F. Rominger, A. S. K. Hashmi, *Adv. Synth. Catal.* **2017**, *359*, 1637–1642; c) S. Tavakkolifard, K. Sekine, L. Reichert, M. Ebrahimi, K. Museridz, E. Michel, F. Rominger, R. Babaahmadi, A. Ariafard, B. F. Yates, M. Rudolph, A. S. K. Hashmi, *Chem. Eur. J.* **2019**, *25*, 12180–12186; d) V. Weingand, T. Wurm, V. Vethacke, M. C. Dieltl, D. Ehjeij, M. Rudolph, F. Rominger, J. Xie, A. S. K. Hashmi, *Chem. Eur. J.* **2018**, *24*, 3725–3728; e) V. Claus, M. Schukin, S. Harrer, M. Rudolph, F. Rominger, A. M. Asiri, J. Xie, A. S. K. Hashmi, *Angew. Chem.* **2018**, *130*, 13148–13152; *Angew. Chem. Int. Ed.* **2018**, *57*, 12966–12970; f) K. Sekine, F. Stuck, J. Schulmeister, T. Wurm, D. Zetschok, F. Rominger, M. Rudolph, A. S. K. Hashmi, *Chem. Eur. J.* **2018**, *24*, 12515–12518; g) A. Ahrens, J. Schwarz, D. M. Lustosa, R. Pourkaveh, M. Hoffmann, F. Rominger, M. Rudolph, A. Dreuw, A. S. K. Hashmi, *Chem. Eur. J.* **2020**, *26*, 5280–5287.
- [6] a) M. Kreuzahler, G. Haberhauer, *Angew. Chem.* **2020**, *132*, 9519–9524; *Angew. Chem. Int. Ed.* **2020**, *59*, 9433–9437; for a related dimerization reaction of chloroalkynes, see: b) M. Kreuzahler, A. Daniels, C. Wölper, G. Haberhauer, *J. Am. Chem. Soc.* **2019**, *141*, 1337–1348.
- [7] For the reactions using ynamides, see: a) W. Xu, G. Wang, X. Xie, Y. Liu, *Org. Lett.* **2018**, *20*, 3273–3277; b) B. Prabagar, S. Dutta, V. Gandon, A. K. Sahoo, *Asian J. Org. Chem.* **2019**, *8*, 1128–1132; for a review, see: c) F. Pan, C. Shu, L.-W. Ye, *Org. Biomol. Chem.* **2016**, *14*, 9456–9465.
- [8] For vinyl cation formation by nucleophilic attack of alkyne to gold carbenoid generated using *N*-oxides, see: a) Z. Zheng, L. Zhang, *Org. Chem. Front.* **2015**, *2*, 1556–1560; b) K. Ji, X. Liu, B. Du, F. Yang, J. Gao, *Chem. Commun.* **2015**, *51*, 10318–10321; for a review, see: c) S. P. Sancheti, N. T. Patil, *Eur. J. Org. Chem.* **2021**, 1321–1330.
- [9] For a review on gold vinylidene intermediates, see: a) A. S. K. Hashmi, *Acc. Chem. Res.* **2014**, *47*, 864–876; b) F. Gagosz, *Synthesis* **2019**, *51*, 1087–1099; c) S. W. Roh, K. Choi, C. Lee, *Chem. Rev.* **2019**, *119*, 4293–4356.
- [10] For a review on gold-catalyzed hydroamination of alkynes, see: a) N. T. Patil, V. Singh, *J. Organomet. Chem.* **2011**, *696*, 419–432; b) W. Debrouwer, T. S. A. Heugebaert, B. I. Roman, C. V. Stevensa, *Adv. Synth. Catal.* **2015**, *357*, 2975–3006.
- [11] T. Ikeuchi, S. Inuki, S. Oishi, H. Ohno, *Angew. Chem.* **2019**, *131*, 7874–7878; *Angew. Chem. Int. Ed.* **2019**, *58*, 7792–7796.
- [12] For the reactions of allenynes for the construction of fused rings, see: a) G. Lemièrre, V. Gandon, N. Agenet, J. P. Goddard, A. Kozak, C. Aubert, L. Fensterbank, M. Malacria, *Angew. Chem.* **2006**, *118*, 7758–7761; *Angew. Chem. Int. Ed.* **2006**, *45*, 7596–7599; b) G.-Y. Lin, C.-Y. Yang, R.-S. Liu, *J. Org. Chem.* **2007**, *72*, 6753–6757; c) R. Zriba, V. Gandon, C. Aubert, L. Fensterbank, M. Malacria, *Chem. Eur. J.* **2008**, *14*, 1482–1491; d) X. Chen, Y. Zhou, J. Jin, K. Farshadfar, A. Ariafard, W. Rao, P. W. H. Chan, *Adv. Synth. Catal.* **2020**, *362*, 1084–1095; e) X. Chen, X. Ling, D. An, W. Rao, *Eur. J. Org. Chem.* **2020**, 5227–5233.
- [13] a) H. Liu, Y. Jia, *Nat. Prod. Rep.* **2017**, *34*, 411–432; b) Y. Hua, Z.-Y. Chen, H. Diao, L. Zhang, G. Qiu, X. Gao, H. Zhou, *J. Org. Chem.* **2020**, *85*, 9614–9621; c) S. Rej, N. Chatani, *Chem. Eur. J.* **2020**, *26*, 11093–11098.
- [14] M. Stepień, E. Gońka, M. Żyła, N. Sprutta, *Chem. Rev.* **2017**, *117*, 3479–3716.
- [15] V. Guilarte, M. P. Castroviejo, P. García-García, M. A. Fernández-Rodríguez, R. Sanz, *J. Org. Chem.* **2011**, *76*, 3416–3437.
- [16] a) A. G. Myers, M. Movassaghi, B. Zheng, *J. Am. Chem. Soc.*, **1997**, *119*, 8572–8573; b) M. Movassaghi, O. K. Ahmad, *J. Org. Chem.* **2007**, *72*, 1838–1841.
- [17] It cannot be completely ruled out that the allene **6** is an intermediate for other substrates with a different protecting group. However, since the products **5b** and **5d** (and their oxidized congeners **10**) were not detected in the reaction mixture shown in Scheme 5, it is unlikely that the allenes **6b** and **6d** are the reactive intermediates for the bis-cyclization products.
- [18] The importance of the silver salt in the isomerization step was confirmed by the following experiments: crude **4a** was obtained by treatment of **3a** with the optimized catalyst for a shorter reaction time followed by short column chromatography. Whereas the silver-free gold catalyst **L2AuNTf₂** (5 mol%) only produced a small amount of the isomerization product **5a** (<5%) after 24 h, AgNTf₂ almost completed isomerized **4a** to **5a** within 5 h.



- [19] For a recent review on additive effects, see: a) Z. Lu, T. Li, S. R. Mudshinge, B. Xu, G. B. Hammond, *Chem. Rev.* **2021**, *121*, 8452–8477; for protodeauration, see: b) W. Wang, M. Kumar, G. B. Hammond, B. Xu, *Org. Lett.* **2014**, *16*, 636–639; c) R. BabaAhmadi, P. Ghanbari, N. A. Rajabi, A. S. K. Hashmi, B. F. Yates, A. Ariafard, *Organometallics* **2015**, *34*, 3186–3195.
- [20] Both ¹H NMR (DCE-*d*₄ at 60 °C) and DFT calculations of **3a** and **3g** strongly indicated the formation of an intramolecular hydrogen bond as shown below, although no definitive evidence for the effect of the hydrogen bonding on the selectivity and reactivity of the cyclization reactions has been obtained at this moment. See the Supporting Information for details.

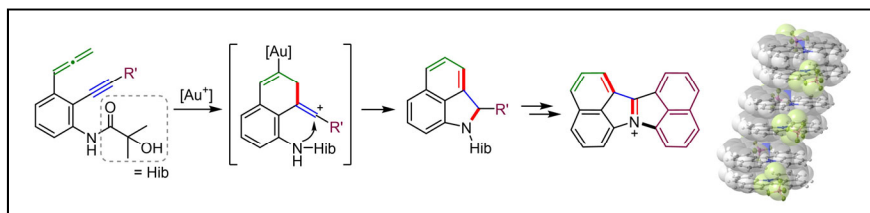


- [21] 4*H*-Benzo[*def*]carbazole has high electron-donating ability, which has potential for applications as a material for organic LEDs and solar cells. See: a) Z. M. Geng, K. Shibasaki, M. Kijima, *Synth. Met.* **2016**, *213*, 57–64; b) Z. M. Geng, T. Yasuda, M. Kijima, *Synth. Met.* **2016**, *220*, 440–447.
- [22] H.-F. Chang, B. P. Cho, *J. Org. Chem.* **1999**, *64*, 9051–9056.
- [23] For examples of synthesis of 4*H*-benzo[*def*]carbazoles, see: a) G. Grigoleit, O. Kruber, *Chem. Ber.* **1954**, *87*, 1895–1905; b) V. R. Kreher, W. Gerhardt, *Angew. Chem.* **1975**, *87*, 288–289; c) T. Horaguchi, R. Yamazaki, T. Abe, *Bull. Chem. Soc. Jpn.* **1980**, *53*, 494–497; d) T. Horaguchi, T. Oyanagi, *J. Heterocyclic Chem.* **2004**, *41*, 1–6; e) Z. He, C. Zhang, X. Xu, L. Zhang, L. Huang, J. Chen, H. Wu, Y. Cao, *Adv. Mater.* **2011**, *23*, 3086–3089.
- [24] Unfortunately, attempted transformation of **12b** to produce **12a** via elimination has not been successful.
- [25] K. Asai, A. Fukazawa, S. Yamaguchi, *Chem. Eur. J.* **2016**, *22*, 17571–17575.

RESEARCH ARTICLE

- [26] A. Bondi, *J. Phys. Chem.* **1964**, *68*, 441–451.
- [27] B. Jeziorski, R. Moszynski, K. Szalewicz, *Chem. Rev.* **1994**, *94*, 1887–1930.
- [28] C. D. Sherrill *et al.*, *J. Chem. Theory Comput.* **2017**, *13*, 3185–3197.
- [29] According to the rate constants for the radiative (k_r) and nonradiative decay processes (k_{nr}), which were calculated based on the values of Φ_f and fluorescence lifetime τ (Table 3), the k_{nr} values of **21** in higher-concentration ($8.1 \times 10^7 \text{ s}^{-1}$) are about significantly smaller than that in the lower-concentration ($3.4 \times 10^8 \text{ s}^{-1}$), while the k_r values are comparable each other ($1.2 \times 10^7 \text{ s}^{-1}$ and $3.3 \times 10^7 \text{ s}^{-1}$ for $1.0 \times 10^{-4} \text{ M}$ and $1.0 \times 10^{-6} \text{ M}$, respectively). These results indicate that the enhancement of fluorescence quantum yield Φ_f of **21** in higher concentration is mainly attributable to the suppression of nonradiative decay processes.

Entry for the Table of Contents



The gold-catalyzed biscyclization of hydroxyisobutyryl (Hib)-protected aminoallenes was promoted by BrettPhosAuNTf₂ in the presence of *i*PrOH to give 1,2-dihydrobenzo[*cd*]indole derivatives, some of which were converted into nitrogen-containing polycyclic aromatic compounds with highly conjugated π -electron systems. A hexacyclic indolium salt (see structure) showed concentration-dependent photophysical properties attributable to aggregate formation